ANATOMICAL CONNECTIVITY MAPPING QUANTIFIES NEUROPLASTIC ACTIVITY OF ANTICHOLINESTERASE TREATMENTS IN PATIENTS WITH AD

M. Bozzali[1], T. Gili[2,3], L. Serra[1], B. Maraviglia[1,3], C. Caltagirone[4,5], K. Embleton[6], G. J. Parker[7], and M. Cercignani[1]

[1]Neuorimaging Laboratory, Santa Lucia Foundation, Rome, Italy, [2]MarbiLab, Enrico Fermi Centre, Rome, Italy, [3]Dept of Physics, University of Rome "La Sapienza", Rome, Italy, [4]Department of Clinical and Behavioural Neurology, Santa Lucia Foundation, Rome, Italy, [5]Dept of Neuroscience, University of Rome "Tor Vergata", [6]Cognition and Cognitive Neuroscience Group, School of Psychological Sciences, University of Manchester, United Kingdom, [7]Imaging Science & Biomedical Engineering and the Biomedical Imaging Institute, University of Manchester, United Kingdom

Introduction

Previous neuroimaging studies have shown inconsistent distributions between volumetric (1,2) and functional changes (3,4) in AD brains. These findings suggest that the clinical manifestations of AD are not only associated with regional GM damage, but also with abnormal functional integration of different brain regions by disconnection mechanism. Recently, a measure of anatomical connectivity derived from diffusion MRI tractography has been proposed (5). Anatomical connectivity mapping (ACM) is obtained by initiating streamlines from all parenchymal voxels, and then counting the number of streamlines passing through each voxel of the brain. We assessed WM structural connectivity based on ACM in a group of patients with AD, in a group of patients with amnestic mild cognitive impairment (aMCI, which is considered the prodromal stage of AD) and in a group of healthy controls, in order to investigate whether structural connectivity is altered in AD.

Methods

Nine patients with moderate AD (F/M=6/3, mean age [SD]= 72.4 [4.5] yrs), 16 patients with aMCI (F/M=6/10, mean age [SD]=72.6 [6.5] yrs) and 12 healthy controls (F/M=3/9, mean age [SD]= 64.8 [10.6] yrs) have been recruited so far for this study. All patients and controls were tested with an extensive neuropsychological battery. Seven out of 9 patients with AD, but none of those with aMCI, were under medication with cholinesterase inhibitors (6 with donepezil and 1 with rivastigmine). Diffusion MRI data were obtained at 3T using a twice-refocused spin echo EPI (TR= 7 s, TE=85 ms, 61 diffusion directions, maximum b factor=1000 smm^{-2}, isotropic resolution 2.3mm^3). All subjects had also a T1-weighetd 3D MDEFT (TR = 1338 ms, TE = 2,4 ms, Matrix = 256 x 224, n. slices = 176, thick. 1 mm), which was coregistered with diffusion data and segmented into WM, grey matter and CSF using SPM8 (www.fil.ion.ucl.ac.uk/spm/). A binary parenchymal mask was obtained by combining grey and white matter segments and retaining only voxels with intensity greater than 0.8 on the resulting image. Diffusion data were first corrected for eddy current induced distortion using a tool from FSL (www.fmrib.ox.ac.uk/fsl/). All the remaining processing was done using Camino (www.camino.org.uk/), if not otherwise specified. The diffusion tensor was estimated in every voxel, and maps of FA were obtained for every subject. The intra-voxel fibre orientation distribution functions (ODFs) and the principal directions of diffusion (with a maximum of 3 per voxel) were reconstructed in every voxel using Q-ball (6). Probabilistic tractography using the probabilistic index of connectivity (PICo, 7) with 10 Monte Carlo iterations was initiated from all voxels in the parenchymal mask. ACMs were obtained by counting the total number of streamlines passing through each voxel and normalised it by the total number of streamlines initiated. ACM and FA images were normalised into MNI space using the transformation obtained during the segmentation step, and smoothed with 8 mm^3 FWHM Gaussian filter. A voxel-wise statistical comparison (adjusted for age and gender) between groups was performed using SPM8. For the ACM comparison, the analysis was also adjusted for the total number of parenchymal voxels in the seed mask.

Results

Fig 1 shows an example of ACM (bottom), together with the corresponding FA map (top). FA was **reduced** in aMCI patients in the precuneus compared to healthy controls. No ACM differences were found between patients with aMCI and healthy controls in either direction. When comparing patients with AD and healthy controls, FA was found to be **reduced** in the thalamus, in the splenium of the corpus callosum and in the anterior cingulate gyrus (Fig 2A). None of these areas survived family-wise error (FWE) correction. No areas of **reduced** ACM were found in the AD group, while areas of **increased** ACM were observed in the putamen and pallidum (bilaterally), in the white matter adjacent to the left insular cortex, in the corpus callosum/posterior cingulum area, in the right central opercular cortex, and in the right lateral occipital cortex (see Fig 2B). After correction for multiple comparison (FWE, $p<0.05$) the only surviving cluster was that located in the left putamen. The mean ACM value from the clusters shown in Fig 2B was extracted and plotted against scores from the mini-mental state examination (MMSE, an index of global cognitive performance) in patients only (both aMCI and AD). Strong inverse associations were found in all regions (see posterior cingulate example in fig 3).

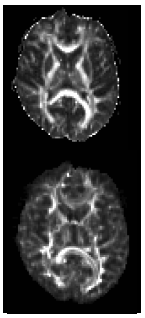

Fig 1. FA (top) and ACM (bottom).

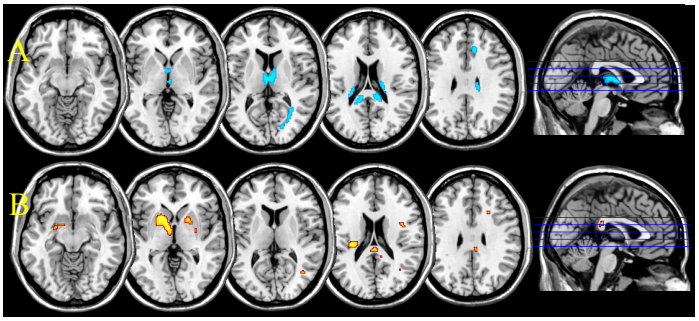

Fig 2. Results of the statistical comparison of FA with the contrast AD<healthy controls (A) and of the statistical comparison of ACM with the opposite contrast, AD>healthy controls (B).

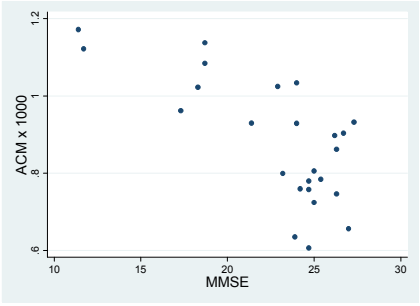

Fig 3. Scatterplot of ACM of the posterior cingulate vs MMSE of all patients. The same pattern was observed in all regions where AD had greater ACM than controls

Discussion

The regional increase in ACM found in patients with AD is unexpected, as previous diffusion studies suggest a progressive brain disconnection across AD evolution (2). Nonetheless, regional ACM was strictly associated with patients' MMSE score, which is an independent clinical measure of AD progression. In this perspective, ACM provides information on brain tissue characteristics that is complementary to that measured by FA, whose decrease is widely believed to reflect axonal damage and loss. We are still investigating the causes of the observed differences. Given that the regions of increased ACM we observed in AD patients were mainly distributed in sub-cortical regions, including the basal forebrain, which is (with the nucleus of Maynert) the major source of cholinergic efferents to the cerebral cortex, one intriguing possibility is the regional increase of ACM in AD patients (only) might reflect processes of brain plasticity driven by cholinesterase inhibitors. These medications are known to play a symptomatic effect in AD by acetylcholine (Ach) replacement. In addition, there is experimental evidence (8) that Ach has also neurotrophic and neurorestorative properties on the cholinergic neurons, thus mitigating the effects of neurodegeneration. If this was the case, an increased number of regenerating axons and sprouting of collateral fibres might result in an increase of ACM, and in a concomitant FA reduction within the same voxels. The generation of axons could also lead to "unmasking" of pathways previously hard to detect with tractography. Moreover, mechanisms of brain plasticity are also believed to occur spontaneously in brains affected by AD. These conclusions, however, should be considered as speculative, as ACM is a novel method of analysis of diffusion MRI and deserves some more investigations. It is also important to emphasise that ACM reflects the total set of anatomical connections to a given voxel, so differences observed in a specific area may be due to the integrated effect of alterations in other connected regions. Future work should look also at correlations between ACM and the duration/dosage of treatment with cholinesterase inhibitors.

References

1. Bozzali M et al., (2006) Neurology;67:453-60 ; 2. Serra L et al., (2009) J Alzheimers Dis; in press ; 3. Kawachi T et al., (2006) Eur. J. Nucl Med Mol Imaging;33:801-9; 4. Matsuda et al., (2002) J Nucl Med;43,304-11 ; 5. Embleton K et al., (2007) . ISMRM 2007, 1548 ; 6. Tuch DS., (2004) Magn Reson Med 52:1358; 7. Parker GJ, et al. (2003). J Magn Reson Imaging; 18:242; 8. Ginestet L et al., (2007) J Neurochem;102:434-40